Scientia Iranica A (2019) 26(5), 2678–2688

SCIENTIA
IRANICA

Sharif University of Technology
Scientia Iranica
Transactions A: Civil Engineering
http://scientiairanica.sharif.edu

Soft computing-based approach for capacity prediction of FRP-strengthened RC joints

M.H. Ilkhani, H. Naderpour*, and A. Kheyroddin

Faculty of Civil Engineering, Semnan University, Semnan, Iran.

Received 13 May 2017; received in revised form 21 August 2017; accepted 5 February 2018

KEYWORDS
RC Joint;
FRP;
Capacity;
ANN.

Abstract. Shear failure of RC beam-column joints is a brittle failure that occurs with no prior warning and induces tremendous damages due to collapse of column and joint before the connected beam. This paper is focused on one particular method of strengthening the RC joints, that is, the use of FRP composites as a confining element. The results of previous studies have shown that strengthening the RC beam-column joints with FRP composites could improve their shear capacity. In this study, the data collected from the existing standards and studies regarding the FRP strengthened RC joints were used to develop an artificial neural network model to predict the shear strength contribution of FRP jacket. The developed model was then used to evaluate the role of different parameters in this contribution and, finally, derive a formula to contribute FRP jacket to the shear strength of the RC beam-column joints.

1. Introduction

The idea of using Fibe-Reinforced Polymer (FRP) composites as a confining component was first introduced by Fardis and Khalili in 1982 [1]. Later, this idea was developed through laboratory and analytical works of other researchers; for instance, Lee and Fenves used FRP jacket for shear and flexural strengthening of joints [2]; Antonopoulos and Triantafillou studied the use of Fiber-Reinforced Polymer (FRP) composites for strengthening beam-column joints while taking the role of fiber debonding into account [3]; Parvin and Granata [4,5] studied the effect of FRP on RC joints through computer modeling as well as laboratory work. These studies have been generally focused on augmenting the shear strength.

The effectiveness of FRP for shear strengthening of RC joints is associated with multiple factors including dimensions of joint, elasticity modulus of composite material, etc. Considering the complexity of shear failure mechanism and the multitude of parameters affecting the shear capacity of FRP jacket, the use of Artificial Neural Networks (ANN) could be a good solution for finding the relationships between these parameters and their effect on shear strength contribution of FRP component. In this study, an ANN model is developed to predict the shear strength contribution of FRP jacket to shear-strengthened RC joints.

2. Artificial neural network

Artificial Neural Network (ANN) is an intelligent system with extensive applications in science and engineering since the late 1980s. ANNs can be described as an extremely simple electronic model of the human brain. Learning mechanisms of the brain are based primarily on experience, and the extraordinary power of the brain to absorb these experiences originates

*. *Corresponding author. Tel.: +98 23 33533781;*
Fax: +98 23 33654121
E-mail address: naderpour@semnan.ac.ir (H. Naderpour)

doi: 10.24200/sci.2018.20177

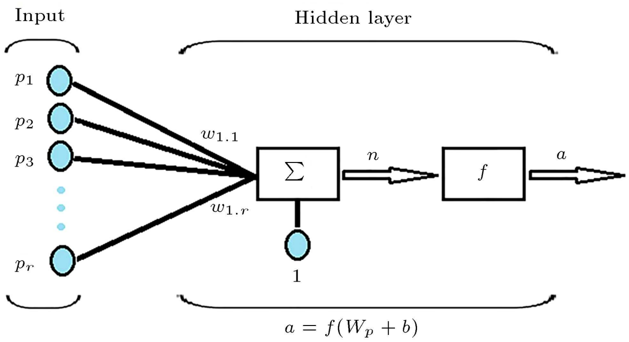

Figure 1. Typical computational models of artificial neural networks (p = input vector, w = input variables weight, n = internal processing function, f = activation function, and a = output vector).

from the presence of a tremendous number of neurons and their natural connections. The core principles of ANN models are based on a similar logic [6-11]. A schematic representation of neurons in a network is shown in Figure 1. Application of ANNs in predicting the response of structural elements has been considered by some researchers [12-19].

2.1. ANNs' input parameters

This study was performed using a set of empirical data regarding the FRP-strengthened RC joints. In all collected data, shear strength contribution of FRP was obtained through the following procedure. First, in each experiment, at least one control specimen was used to determine the baseline shear strength of the joint. This baseline shear strength is the sum of shear strength contribution of concrete and that of steel stirrups (when present). Next, the shear strengths of the FRP-strengthened specimens identical to the control specimens were obtained. Finally, the shear strength contribution of FRP was obtained by subtracting the baseline shear strength from the shear strength of the corresponding FRP-strengthened specimen.

Initially, data pertaining to 155 FRP-strengthened joint specimens were collected [20-51]. Of these 155 specimens, 34 specimens had shown debonding during the test and could not be used. In addition, 55 specimens had an undesirable mechanism of failure (failure in beam before FRP reaching its capacity in the joint) and were, therefore, removed from the data. The use of such data instances in the network training leads to error, because the joint specimen fails before reaching its maximum shear capacity, meaning that it would have sustained a greater shear force if the beam had a greater shear capacity. In addition, 8 specimens were also strengthened with other types of reinforcement and were, therefore, removed from the data to ensure the uniformity of inputs. Therefore, ultimately, 58 specimens remained for analysis.

After collecting suitable data for the network, it is required to choose the parameters that affect the output values. After reviewing the literature [52,53], it was concluded that shear strength contribution of FRP was influenced by the six following parameters:

- Effective depth of the FRP on the joint and the angle between the axis of the column and fiber orientation, D (mm);
- Cross-sectional area of the column, A_c (mm^2);
- Compressive strength of the concrete, f'_c (MPa);
- Elasticity modulus of the FRP, E (GPa);
- Thickness FRP, t_f (mm);
- Tensile strength of the FRP, F_{fu} (MPa).

In this study, shear strength contribution of FRP (V_f) is considered as the output.

Table 1 shows the statistical characteristics of the laboratory specimens used in the networks.

3. Modeling of the artificial neural network

In total, 9 networks with different hidden neurons (2 to 10) were trained. The next step after the training is to identify the best network and, then, to compare its results with the experimental data. The Mean Squared Error (MSE) and regression value of the developed ANNs are shown, respectively, in Figures 2 and 3.

All ANNs were trained using the Levenberg-Maequardt algorithm with back propagation method [54]. The back propagation-based ANNs often use the transfer functions of Log sigmoid and Tan sigmoid. These functions can be used for the output function, which means limiting the output to a small

Table 1. Statistical criteria of experimental data.

Input nodes	f'_c (MPa)	E (GPa)	D_{fu} (MPa)	t_f (mm)	D (mm)	A_c (mm^2)	V_f (kN)
Min	13.5	27.6	135.5	0.053	100	24000	4.12
Max	64.7	285	4965.8	3.3	707.1	148555	69
Average	29.64	175.9	2832.6	0.76	342.7	63124	19.4
Variance	124.8	6729.2	1708859	0.699	22989.8	$1.22^{*}10^{9}$	199.18
Standard deviation	11.17	82.03	1307.2	0.83	151.5	34880.3	14.11

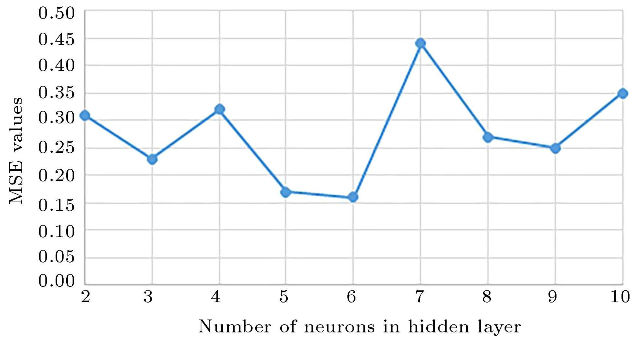

Figure 2. Mean Squared Error (MSE) versus the number of hidden-layer neurons.

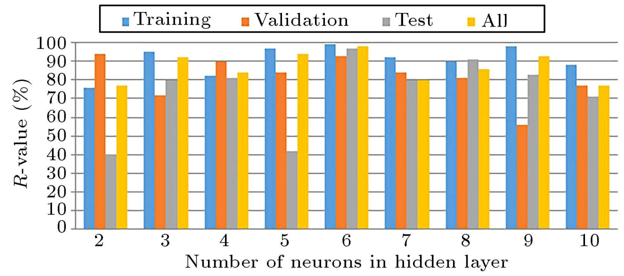

Figure 3. Correlation coefficient versus the number of hidden-layer neuron.

value. The better option for the output function is the Purlin function that allows the output to take any value. The stop condition for training algorithm is the minimization of MSE, that is, the mean squared difference between the output and the target value.

One of the criteria based on which the best ANN can be determined is the regression value. The regression value (R) measures the correlation between the ANN outputs and the target values; $R = 1$ represents a perfect correlation between the output and the target value, while $R = 0$ means that any relationship between the output and the target value would be random. In this study, MSE and regression value were used as the criteria for selecting the ideal network.

As observed, all ANNs were properly trained, and the obtained errors were very small. The highest errors (MSE) were 0.35 and 0.44, which belonged to ANNs with 10 and 7 hidden neurons; the lowest errors were 0.18 and 0.16, observed in ANNs with 5 and 6 hidden neurons. In the most accurate ANNs (those with 5 and 6 hidden neurons), the regression values for the entire data were 94% and 98%. As can be seen, the ANN with 6 hidden neurons had a very good MSE (0.16) and a very high correlation coefficient. The regression values of this ANN for training, verification, test data, and the entire data were 0.999, 0.939, 0.970, and 0.982, respectively. Considering these four criteria, the ANN with 6 hidden neurons was chosen as the best network and the one to be used for the remainder of work.

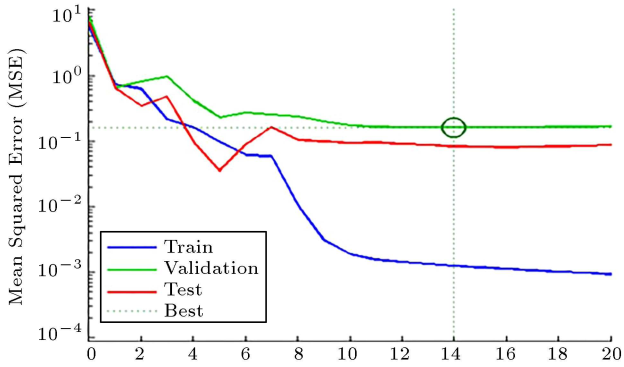

Figure 4. Performance Trained network with 6 neurons in the hidden layer.

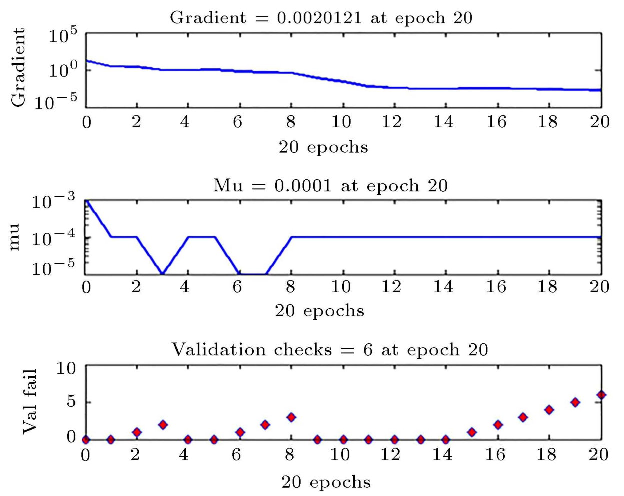

Figure 5. Learning curve networks trained with 6 neurons in the hidden layer.

MSE graph of the ANN with 6 hidden neurons (Figure 4) shows a decreasing trend, representing the network's learning process. This graph has three curves: the MSE for training data, validation data, and test data. At the beginning of the learning, this ANN has an error of about 8%; however, as the learning process continues, network weights are adjusted and errors decrease until reaching down, at the twentieth step, to the values of 0.008, 0.2, and 0.1 for training, validation, and test data.

The graphs illustrating the process of learning, and regressions values of input data are plotted respectively in Figures 5 and 6. A decreasing trend of gradient graph depicted in Figure 5 represents the trend of learning. This gradient reduction continues until MSE reaches down to its minimum value. At this point, learning stops; from this point onwards, gradient is constant. The regression values shown in Figure 6 imply the proper training of the network and demonstrate the close proximity between its outputs and the target vector.

In view of the described results, it was concluded

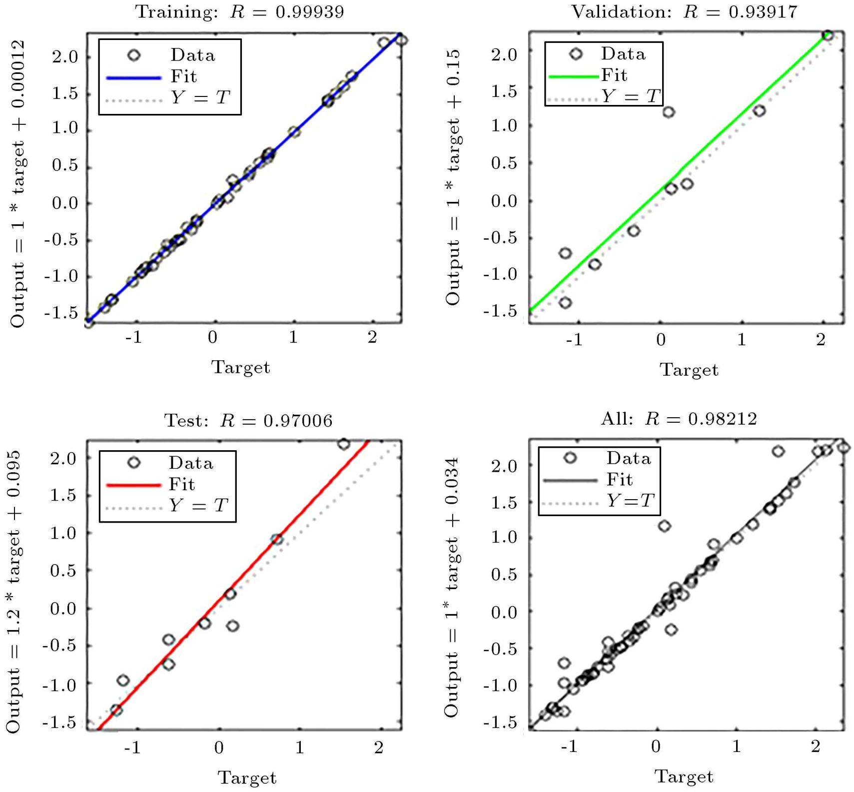

Figure 6. Regression data for training and testing the accuracy of the network with 6 neurons in the hidden layer.

that the ANN modeled with six hidden neurons was properly trained for input and output data, and it is suitable for the remainder of this work.

3.1. *Comparison of the ANN results with experimental data*

To validate the developed ANN, its results were compared with the experimental data. Figure 7 and Table 2 show the relationship between experimentally obtained shear strength contribution of FRP jacket and the value obtained from the developed network. In this figure, the points on the 45-degree line represent zero difference between the experimental data and the results of the proposed formulas; the distance of each point from the 45-degree line represents the magnitude of error in the calculated value.

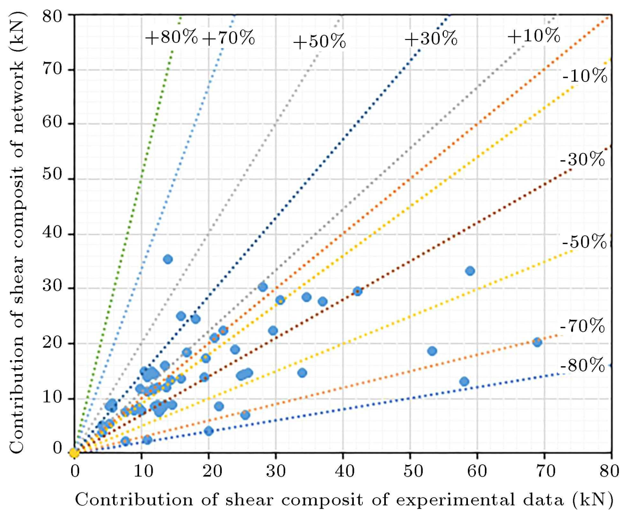

Figure 7. Error compared to the values obtained by neural networks and relationships.

4. The proposed formula for predicting shear strength contribution of FRP component

The above comparisons show the good agreement of the ANN results with the experimental data. However, the direct use of ANN is not a common practice in engineering design; instead, this paper provides a nonlinear relationship capable of predicting the FRP shear strength contribution.

To derive this formula, first, each parameter needs to be initialized with a value (within its variation range). Here, values close to the average values of the parameters were chosen for this purpose. The base values assumed for different variables are shown in Table 3. After determining the base values, one of the six input parameters was considered as a variable, and the range of its variation was divided into several parts. This division needs to include the upper and lower bounds of the variation range as well as the base value.

Table 2. Comparison between errors of the values obtained by neural networks and experimental data.

Range of error (%)	Number of data in the range of error	Percentage of data in the range of error (%)
±10	40	68.9
±20	46	97.3
±30	53	91.3
±40	55	94.8
±60	56	96.5
±130	57	98.2
±220	58	100

Table 3. Range of input parameters and base values for each parameter.

Input nodes	f'_c (MPa)	E (GPa)	F_{fu} (MPa)	t_f (mm)	D (mm)	A_c (mm^2)
Min	13.5	27.6	135.5	0.053	100	24000
Max	64.7	285	4965.8	3.3	707.1	148555
Average	29.64	175.9	2832.6	0.76	342.7	63124.17
Base	30	180	2800	0.75	350	63000
Input correlation	$30/f'_c$	$180/E$	$2800/F_{fu}$	$0.75/T_f$	$350/D$	$63000/A_c$

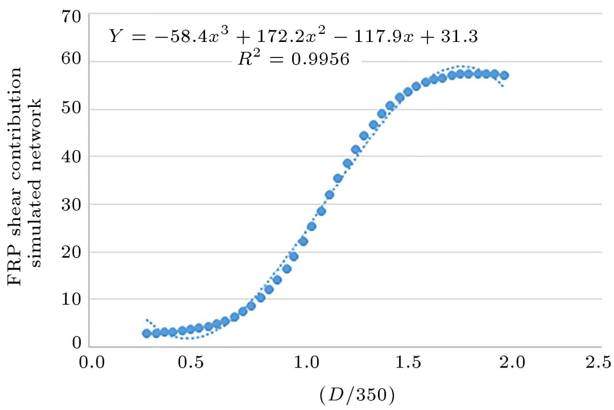

Figure 8. Network output changes in relation to changes in effective (D) with constant five other parameters.

The relationship between the ANN output and parameter (D) was examined. This parameter was chosen because of the low sensitivity shown during the weight analysis. To determine the relationship between the ANN output and parameter (D), the other 5 parameters were initialized with their base values, and (D) was gradually changed from its minimum value to its maximum. The effects of these changes on the ANN output are shown in Figure 8. After determining the relationship between (D) and the ANN output, the same procedure was used to determine the relationship between the output and other 5 parameters.

The algorithm's structure was derived from the algorithm of Leung et al. (2006) for calculating the final strain of FRP in flexural-strengthened beams [55,56].

The resulting model is in the form of Eqs. (1) to (6):

$$V_{\text{equation}} = (C_{f'_c}.C_E.C_{F_{fu}}.C_{T_f}.C_D.C_{A_c}), \tag{1}$$

$$C_{f'_c} = C_{f'_c}(E, F_{fu}, T_f, A_c), \tag{2}$$

$$C_E = C_E(f'_c, F_{fu}, T_f, A_c), \tag{3}$$

$$C_{F_{fu}} = C_{F_{fu}}(E, f'_c, T_f, A_c), \tag{4}$$

$$C_{T_f} = C_{T_f}(E, F_{fu}, f'_c, A_c), \tag{5}$$

$$C_{A_c} = C_{A_c}(E, F_{fu}, T_f, f'_c). \tag{6}$$

To obtain V_f from Eq. (1), six correction factors should be calculated and, then, multiplied by each other. According to Figure 8, C_D can be obtained from Eq. (7).

$$C_D = -58.4 * (\frac{D}{350})^3 + 172.2 * (\frac{D}{350})^2 - 117.9 * (\frac{D}{350})^2 + 31.3. \tag{7}$$

Figures 8 to 28 show the graphs of correction factors of the other 5 parameters.

After averaging the values obtained for each parameter, the correction factors are determined as follows:

$$C_{f'_c} = 0.535 * (\frac{f'_c}{30}) + 0.25, \tag{8}$$

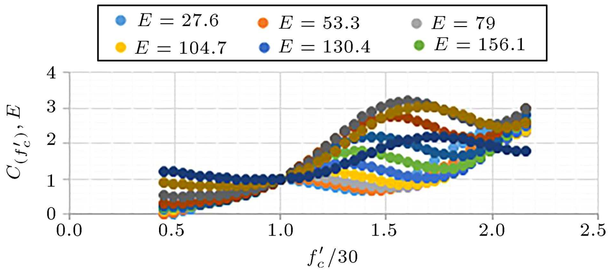

Figure 9. Change ratio E of correction coefficient $C_{f'c}$.

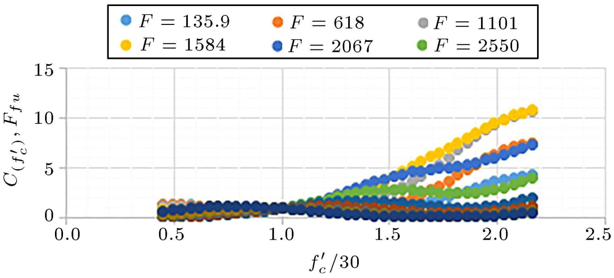

Figure 10. Change ratio F_{fu} of correction coefficient $C_{f'c}$.

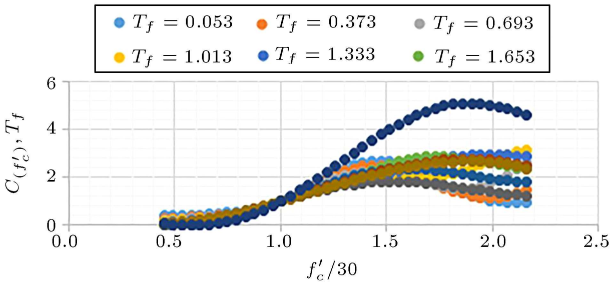

Figure 11. Change ratio T_f of correction coefficient $C_{f'c}$.

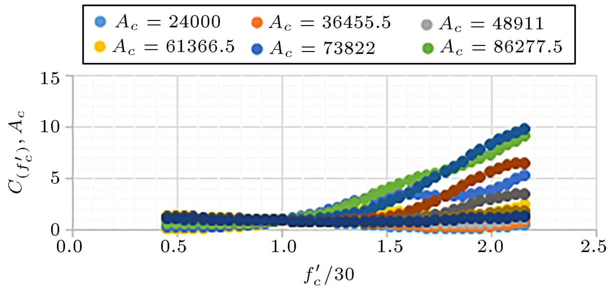

Figure 12. Change ratio A_c of correction coefficient $C_{f'c}$.

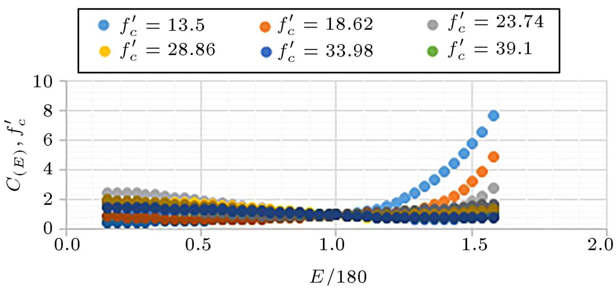

Figure 13. Change ratio f'_c of correction coefficient C_E.

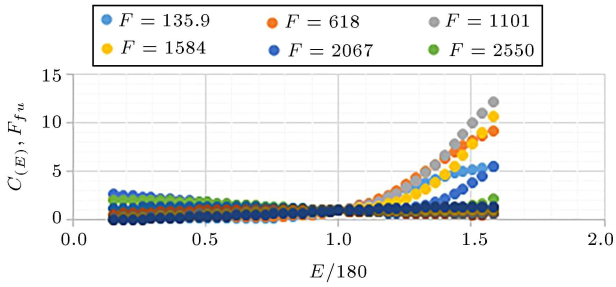

Figure 14. Change ratio F_{fu} of correction coefficient C_E.

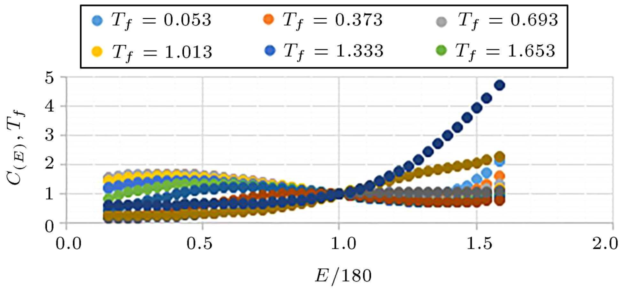

Figure 15. Change ratio T_f of correction coefficient C_E.

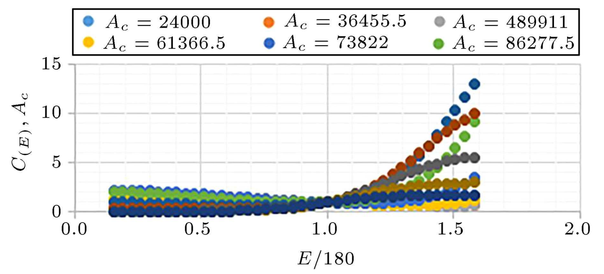

Figure 16. Change ratio A_c of correction coefficient C_E.

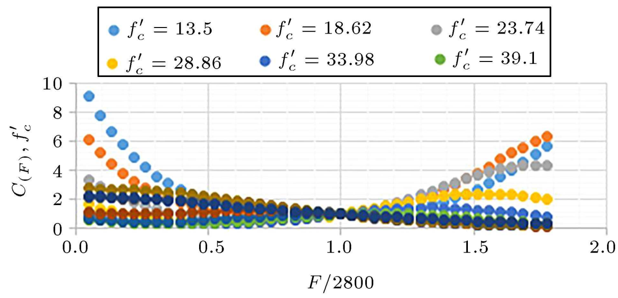

Figure 17. Change ratio f'_c of correction coefficient C_{Ffu}.

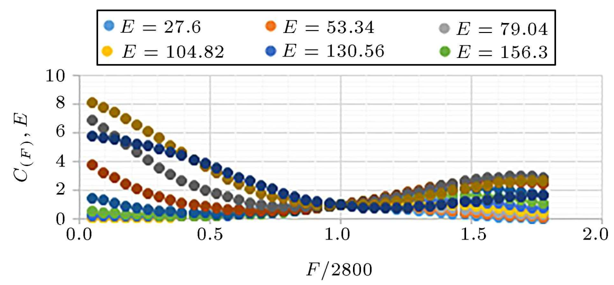

Figure 18. Change ratio E of correction coefficient C_{Ffu}.

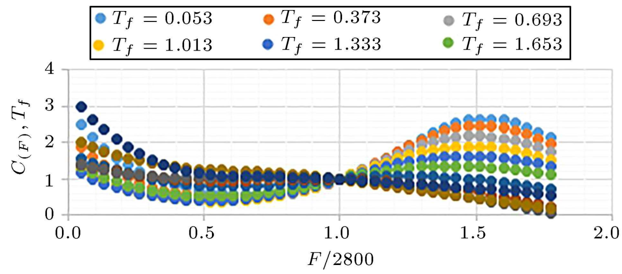

Figure 19. Change ratio T_f of correction coefficient C_{Ffu}.

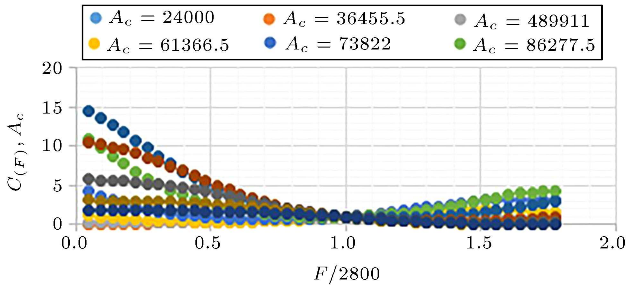

Figure 20. Change ratio A_c of correction coefficient C_{Ffu}.

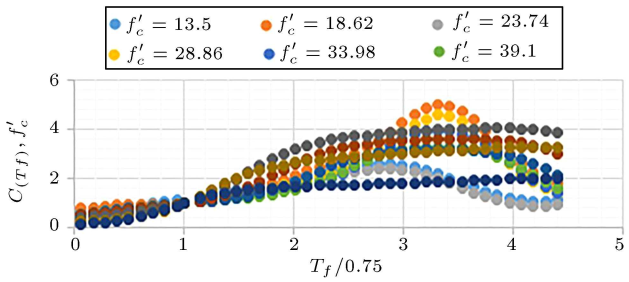

Figure 21. Change ratio $f'c$ of correction coefficient C_{Tf}.

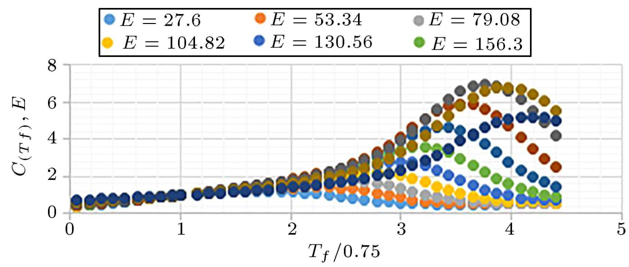

Figure 22. Change ratio E of correction coefficient C_{Tf}.

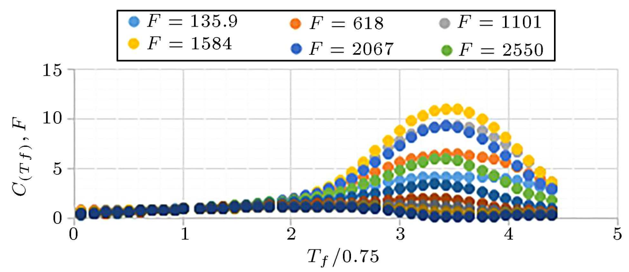

Figure 23. Change ratio F_{fu} of correction coefficient C_{Tf}.

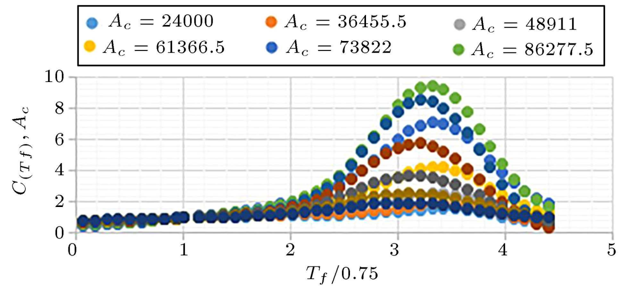

Figure 24. Change ratio A_c of correction coefficient C_{Tf}.

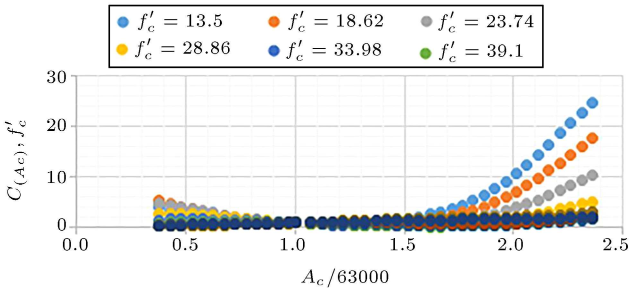

Figure 25. Change ratio $f'c$ of correction coefficient C_{Ac}.

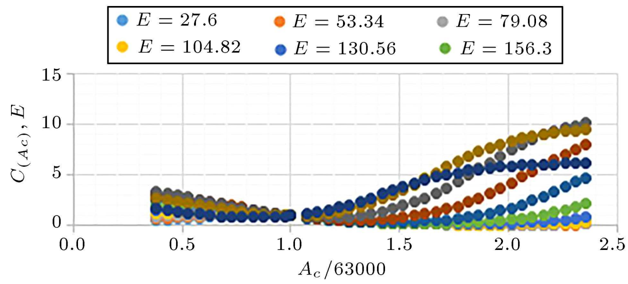

Figure 26. Change ratio E of correction coefficient C_{Ac}.

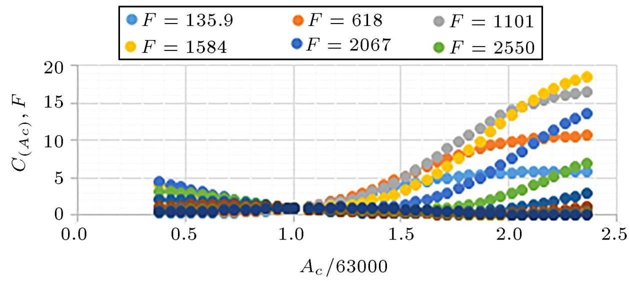

Figure 27. Change ratio F_{fu} of correction coefficient C_{Ac}.

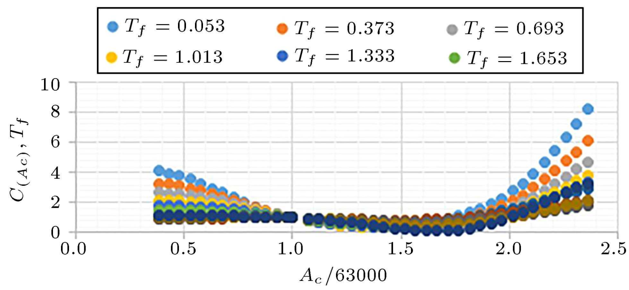

Figure 28. Change ratio T_f of correction coefficient C_{Ac}.

$$C_E = 1.995 * (\frac{E}{180})^3 - 3.65 * (\frac{E}{180})^2 + 2 * (\frac{E}{180}) + 0.54, \tag{9}$$

$$C_{F_{fu}} = 0.64 * (\frac{F_{fu}}{2800})^3 - 1.99 * (\frac{F_{fu}}{2800})^2 + 2.07 * (\frac{F_{fu}}{2800}) + 0.355, \tag{10}$$

$$C_{T_f} = 0.1 * (\frac{T_f}{0.75}) + 0.82, \tag{11}$$

$$C_{A_c} = 0.515 * (\frac{A_c}{63000})^3 - 2.3 * (\frac{A_c}{63000})^2 + 3.2 * (\frac{A_c}{63000}) - 0.45. \tag{12}$$

The errors in FRP shear strength contribution obtained by the proposed formulas are shown in Table 4. Figure 29 shows the relationship between the experimental data and those obtained by the proposed formulas. In this figure, the points on the 45-degree line represent zero difference between the experimental data and the results of the proposed formulas; each point's distance from the 45-degree line represents the magnitude of error in calculated value.

As the graph of Figure 29 shows, most points obtained by the proposed formula are positioned near the bisector line, which indicates the good ability of this formula to predict the shear strength contribution of FRP component.

5. Statistical results of the proposed formula

In this section, a number of statistical criteria for the error of the proposed formula to predict FRP shear strength contribution are examined.

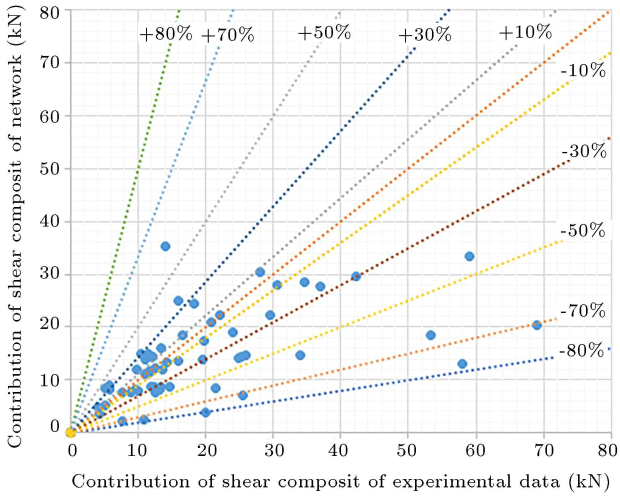

Figure 29. Comparison of experimental results with predicted values by the proposed equation.

5.1. *Average error (e_{Avg})*

The average error of the proposed formula was calculated using Eq. (13), and the value of this criterion for 58 available data instances was calculated as 33.3%.

$$\bar{e} = \frac{\sum_{i=1}^{N} (v_i - v_{it})}{N}. \tag{13}$$

5.2. *Standard deviation*

This criterion can express the dispersion of results compared to the mean values. Eq. (14) gives the variance for the proposed formula, and the root of this parameter is the standard deviation. The standard deviation of the proposed formula is 8.02%, which indicates the low dispersion of its results.

$$\text{var} = \frac{\sum_{i=1}^{N} (v_i - \bar{v})^2}{N}. \tag{14}$$

Table 4. Error values obtained by the proposed equations.

Range of error (%)	Number of error data in the proposed equations	Percentage error of data in the proposed equations (%)
±10	11	18.9
±20	21	36.2
±30	32	55.1
±40	38	65.5
±50	45	77.5
±60	47	81
±70	51	87.9
±80	56	96.5
±90	57	98.2
±160	58	100

5.3. Root Mean Square Error (RMSE)

The other criterion used to measure the error of the proposed formula is the Root Mean Square Error (RMSE); the smaller the values of RMSE, the lower the error of theoretical results, as compared to experimental data. Through Eq. (15), the value of this criterion for the proposed formula was calculated as 14.88%, indicating the good accuracy of the proposed formula:

$$RMSE = \sqrt{\frac{\sum_{i=1}^{N} (v_i - v_{it})^2}{N}}. \qquad (15)$$

6. Conclusion

In this paper, first, the previous studies on the shear capacity of the FRP-strengthened RC joints were reviewed. The shear strength contribution of FRP to the RC joints can be influenced by many factors, and given the complex mechanism and danger of shear failure, estimating this contribution is of significant importance in preventing early shear failure of the column before the beam. It was concluded that shear strength contribution of FRP was influenced by the six following parameters: effective depth of the FRP in the joint and the angle between the axis of the column and fiber orientation, cross-sectional area of the column, compressive strength of the concrete, modulus of elasticity of the FRP, thickness FRP, and tensile strength of the FRP. Furthermore, shear strength contribution of FRP was considered as the output. In addition, the authors attempted to provide a formula for estimating the shear strength contribution of FRP jacket.

Artificial neural networks provided a general practical method for real-valued, discrete-valued, and vector-valued functions from examples; therefore, they have been widely used in the various applications of engineering fields.

Finally, the artificial neural network architecture was used to develop a model for predicting the FRP shear strength contribution, and the developed model was then used to derive a formula for estimating the shear force sustained solely by the FRP jacket in the RC joint. In the end, the results of the proposed formula were compared with the experimental data. The precision of the proposed equation was verified by the existing experimental data, and a favorable level of agreement was obtained.

References

1. Fardis, M.N. and Khalili, H.H. "FRP-encased concrete as a structural material", *Magazine of Concrete Research*, **34**(121), pp. 191-202 (1982).
2. Lee, J. and Fenves, G.L. "Plastic-damage model for cyclic loading of concrete structures", *Journal of Engineering Mechanics*, **124**(8), pp. 892-900 (1998).
3. Antonopoulos, C.P. and Triantafillou, T.C. "Experimental investigation of FRP-strengthened RC beam-column joints", *Journal of Composites for Construction*, **7**(1), pp. 39-49 (2003).
4. Parvin, A. and Granata, P. "Investigation on the effects of fiber composites at concrete joints", *Composites Part B: Engineering*, **31**(6), pp. 499-509 (2000).
5. Granata, P.J. and Parvin, A. "An experimental study on Kevlar strengthening of beam-column connections", *Composite Structures*, **53**(2), pp. 163-171 (2001).
6. Rosenblatt, F. "The perceptron: A theory of statistical separability in cognitive system", Cornell Aeronautical Lab. Inc. Rep. No. VG-1196-G-1 (1958).
7. Yeung, W.T. and Smith, J.W. "Damage detection in bridges using neural networks for pattern recognition of vibration signatures", *Eng. Struct.*, **27**(5), pp. 685-698 (2005). DOI: 10.1016/j.engstruct.2004.12.006
8. Huang, C.S., Hung, S.L., Wen, C.M., and Tu, T.T. "A neural network approach for structural identification and diagnosis of a building from seismic response data", *Earthq. Eng. Struct. Dyn.*, **32**(2), pp. 187-206 (2003).
9. Neural Network Toolbox for Use with Matlab. User's Guide. Version 3.0. The MathWorks, Inc. (2006).
10. Naderpour, H., Rafiean, A.H., and Fakharian, P. "Compressive strength prediction of environmentally friendly concrete using artificial neural networks", *Journal of Building Engineering*, **16**, pp. 213-219 (2018).
11. Vanajakshi, L. and Rilett, L.R. "A comparison of the performance of artificial neural networks and support vector machines for the prediction of traffic speed", *IEEE Intelligent Vehicles Symposium*, pp. 194-199 (2004).
12. Naderpour, H., Kheyroddin, A., and Amiri, G.G. "Prediction of FRP-confined compressive strength of concrete using artificial neural networks", *Composite Structures*, **92**(12), pp. 2817-2829 (2010).
13. Ahmadi, M., Naderpour, H., and Kheyroddin, A. "Utilization of artificial neural networks to prediction of the capacity of CCFT short columns subject to short term axial load", *Archives of Civil and Mechanical Engineering*, **14**(3), pp. 510-517 (2014).
14. Naderpour, H., Kheyroddin, A., Ghodrati Amiri, G., and Hoseini Vaez, S.R. "Estimating the behavior of FRP-strengthened RC structural members using artificial neural networks", *Procedia Engineering*, **14**, pp. 3183-3190 (2011).
15. Naderpour, H. and Alavi, S.A. "A proposed model to estimate shear contribution of FRP in strengthened RC beams in terms of adaptive neuro-fuzzy inference system", *Composite Structures*, **170**, pp. 215-227 (2017).

16. Ahmadi, M., Naderpour, H., and Kheyroddin, A. "ANN model for predicting the compressive strength of circular steel-confined concrete", *International Journal of Civil Engineering*, **15**(2), pp. 213-221 (2017).

17. Naderpour, H. and Mirrashid, M. "Compressive strength of mortars admixed with wollastonite and microsilica", *Materials Science Forum*, 890 MSF, pp. 415-418 (2017).

18. Naderpour, H., Khatami, S.M., and Barros, R.C. "Prediction of critical distance between two MDOF systems subjected to seismic excitation in terms of artificial neural networks", *Periodica Polytechnica Civil Engineering*, **61**(3), pp. 516-529 (2017).

19. Naderpour, H., Ghodrati Amiri, G., Kheyroddin, A., and Hoseini Vaez, S.R. "Seismic evaluation of retrofitted RC frames using neuro-fuzzy algorithms", *Proceedings of the 8th International Conference on Structural Dynamics*, EURODYN 2011, pp. 446-452 (2011).

20. Akguzel, U. and Pampanin, S. "Effects of variation of axial load and bidirectional loading on seismic performance of GFRP retrofitted reinforced concrete exterior beam-column joints", *Journal of Composites for Construction*, **14**(1), pp. 94-104 (2010).

21. Pantelides, C., Clyde, C., and Reaveley, L. "Rehabilitation of R/C building joints with FRP composites", in *12th World Conference on Earthquake Engineering*, Auckland, New Zealand (2000).

22. Le-Trung, K. "Experimental study of RC beam-column joints strengthened using CFRP composites", *Composites Part B: Engineering*, **41**(1), pp. 76-85 (2010).

23. Mahmoud, M.H., Afefy, H.M., Kassem, N.M., and Fawzy, T.M. "Strengthening of defected beam-column joints using CFRP", *Journal of Advanced Research*, **5**(1), pp. 67-77 (2014).

24. Dalalbashi, A., Eslami, A., and Ronagh, H. "Numerical investigation on the hysteretic behavior of RC joints retrofitted with different CFRP configurations", *Journal of Composites for Construction*, **17**(3), pp. 371-382 (2013).

25. Gergely, J., Pantelides, C.P., and Reaveley, L.D. "Shear strengthening of RCT-joints using CFRP composites", *Journal of Composites for Construction*, **4**(2), pp. 56-64 (2000).

26. Karayannis, C.G. and Sirkelis, G.M. "Strengthening and rehabilitation of RC beam-column joints using carbon-FRP jacketing and epoxy resin injection", *Earthquake Engineering & Structural Dynamics*, **37**(5), pp. 769-790 (2008).

27. Vatani-Oskouei, A. "Repairing of seismically damaged RC exterior beam-column connection using CFRP", *Journal of Reinforced Plastics and Composites*, **29**(21), pp. 3257-3274 (2010).

28. Al-Salloum, Y.A. "Textile-reinforced mortar versus FRP as strengthening material for seismically deficient RC beam-column joints", *Journal of Composites for Construction*, **15**(6), pp. 920-933 (2011).

29. Ha, G.-J. "Seismic improvement of RC beam-column joints using hexagonal CFRP bars combined with CFRP sheets", *Composite Structures*, **95**, pp. 464-470 (2013).

30. Hamad, Bilal S. and Faten, G. Ibrahim "Effect of FRP confinement on bond strength of hooked bars: Normal-strength concrete structures", *Journal of Composites for Construction*, **13**(4), pp. 279-291 (2009).

31. Alsayed, S.H. "Seismic response of FRP-upgraded exterior RC beam-column joints", *Journal of Composites for Construction*, **14**(2), pp. 195-208 (2010).

32. Tsonos, A.G. "Effectiveness of CFRP-jackets and RC-jackets in post-earthquake and pre-earthquake retrofitting of beam-column subassemblages", *Engineering Structures*, **30**(3), pp. 777-793 (2008).

33. Sheela, S. and Anu Geetha, B. "Studies on the performance of RC beam-column joints strengthened using different composite materials", *Journal of the Institution of Engineers (India): Series A*, **93**(1), pp. 63-71 (2012).

34. Kumar, E.S., Murugesan, A., and Thirugnanam, G. "Experimental study on behavior of retrofitted with FRP wrapped RC beam-column exterior joints subjected to cyclic loading", *International Journal of Civil and Structural Engineering*, **1**(1), p. 64 (2010).

35. Ghobarah, A. and El-Amoury, T. "Seismic rehabilitation of deficient exterior concrete frame joints", *Journal of Composites for Construction*, **9**(5), pp. 408-416 (2005).

36. Singh, V. "Experimental studies on strength and ductility of CFRP jacketed reinforced concrete beam-column joints", *Construction and Building Materials*, **55**, pp. 194-201 (2014).

37. Del Vecchio, C. "Experimental investigation of exterior RC beam-column joints retrofitted with FRP systems", *Journal of Composites for Construction*, **18**(4), p. 04014002 (2014).

38. Shrestha, R., Smith, S.T., and Samali, B. "Strengthening RC beam-column connections with FRP strips", Institution of Civil Engineers. Proceedings. Structures and Buildings (2009).

39. Ravi, R.S. and Arulraj, P.G. "Experimental investigation on behavior of reinforced concrete beam column joints retrofitted with GFRP-AFRP hybrid wrapping", *International Journal of Civil and Structural Engineering*, **1**(2), p. 245 (2010).

40. Niroomandi, A. "Seismic performance of ordinary RC frames retrofitted at joints by FRP sheets", *Engineering Structures*, **32**(8), pp. 2326-2336 (2010).

41. Li, B. and Chua, H.G. "Seismic performance of strengthened reinforced concrete beam-column joints using FRP composites", *Journal of Structural Engineering*, **135**(10), pp. 1177-1190 (2009).
42. Masi, A. "Study of the seismic behavior of external RC beam-column joints through experimental tests and numerical simulations", *Engineering Structures*, **52**, pp. 207-219 (2013).
43. Ascione, L. and Berardi, V. "Anchorage device for FRP laminates in the strengthening of concrete structures close to beam-column joints", *Composites Part B: Engineering*, **42**(7), pp. 1840-1850 (2011).
44. Engindeniz, M., Kahn, L.F., and Abdul-Hamid, Z. "Repair and strengthening of reinforced concrete beam-column joints: State of the art", *ACI Structural Journal*, **102**(2), pp. 187-197 (2005).
45. Said, A.M. and Nehdi, M.L. "Use of FRP for RC frames in seismic zones: Part I. Evaluation of FRP beam-column joint rehabilitation techniques", *Applied Composite Materials*, **11**(4), pp. 205-226 (2004).
46. Ghobarah, A. and Said, A. "Seismic rehabilitation of beam-column joints using FRP laminates", *Journal of Earthquake Engineering*, **5**(01), pp. 113-129 (2001).
47. Al-Salloum, Y.A. "Seismic behavior of as-built, ACI-complying, and CFRP-repaired exterior RC beam-column joints", *Journal of Composites for Construction*, **15**(4), pp. 522-534 (2010).
48. Ugale Ashish, B. and Raut Harshalata, R. "Investigation on behaviour of reinforced concrete beam column joints retrofitted with FRP wrapping", *International Journal of Civil Engineering Research*, **5**, pp. 2278-3652 (2014).
49. Gencoglu, M. and Mobasher, B. "The strengthening of the deficient RC exterior beam-column joints using CFRP for seismic excitation", in *Proceedings of the 3 rd International Conference on Structural Engineering, Mechanics and Computation* (2007).
50. Dalalbashi, A., Eslami, A., and Ronagh, H. "Plastic hinge relocation in RC joints as an alternative method of retrofitting using FRP", *Composite Structures*, **94**(8), pp. 2433-2439 (2012).
51. Lee, W.-T., Chiou, Y.-J., and Shih, M. "Reinforced concrete beam-column joint strengthened with carbon fiber reinforced polymer", *Composite Structures*, **92**(1), pp. 48-60 (2010).
52. "Design and use of externally bonded fiber reinforced polymer reinforcement (FRP EBR) for reinforced concrete structures", in FIB Bulletin 14, Lausanne, Switzerland (2001).
53. "Guide for the design and construction of externally bonded FRP systems for strengthening concrete structures", in Rep. No. 440 2R-08, American Concrete Institute (ACI) (2008).
54. Saravanan, J. and Kumaran, G. "Joint shear strength of FRP reinforced concrete beam-column joints", *Central European Journal of Engineering*, **1**(1), pp. 89-102 (2011).
55. Leung, C.K., Ng, M.Y., and Luk, H.C. "Empirical approach for determining ultimate FRP strain in FRP-strengthened concrete beams", *Journal of Composites for Construction*, **10**(2), pp. 125-138 (2006).
56. Ilkhani, M., Moradi, E., and Lavasani, M. "Calculation of torsion capacity of the reinforced concrete beams using artificial neural network", *Soft Computing in Civil Engineering*, **1**(2), pp. 8-18 (2017).

Biographies

Mohammad Hosein Ilkhani was born in Tehran, Iran. He obtained his BS and MS degrees in Civil and Structural Engineering in 2010 and 2014, respectively. His research interests include Neural networks and rehabilitation of concrete members. He is presently a PhD student in Semnan University.

Hosein Naderpour received his PhD degree in Structural Engineering in 2010. He then joined Semnan University where he is presently an Associate Professor of Structural Engineering. Dr. Naderpour is the author of 40 papers published in journals and about 90 papers presented at national and international conferences. He has given several speeches in Japan, Switzerland, China, Australia, Canada, Belgium, Portugal, Spain, Germany, Italy, Czech Republic, and France. His major research interests include application of soft computing in structural engineering, structural reliability, structural optimization, and damage detection of structures.

Ali Kheyroddin received his PhD degree in Structural Engineering in 1996 from McGill University, Canada. He then joined Semnan University where he is presently a Professor of Structural Engineering. His major research interests include analysis and design of tall buildings and HPFRCC technologies.